Macroscopic modeling of functional fatigue in shape memory alloys

Noemi Barrera [a], Paolo Biscari [a,*], Marco Fabrizio Urbano [b]

[a] *Dipartimento di Matematica, Politecnico di Milano, Piazza Leonardo da Vinci 32, 20133 Milan, Italy*
[b] *SAES Getters, Viale Italia 77, 20020 Lainate, Italy*

Received 18 February 2013
Accepted 18 November 2013
Available online 3 December 2013

1. Introduction

Shape memory alloys (or SMA) provide an astonishing combination of fascinating theoretical problems and promising potential industrial applications. From the mathematical point of view, the key element in SMA is the fact that they exhibit a transition between a more symmetric crystallographic phase (*austenite*) to a less symmetric phase (*martensite*) in which the non-trivial and non-convex character of the elastic potential gives rise to a variety of microstructured energy minimizers (Ball and James, 1987). The involved phase transitions (between austenite and martensite, as well as among different martensitic relative energy minimizers, or *variants*) may be controlled by suitably modifying the external temperature and loading conditions. The resulting phase diagrams (Bekker and Brinson, 1998) and the possibility of performing reversible cycles in them (Bhattacharya et al., 2004) are at the basis of potential applications (Otsuka and Ren, 1999; Shabalovskaya et al., 2008).

Several theoretical studies analyze the micro- and macroscopic phenomena consistent with non-convex elastic potentials, basically derived from the analysis of the symmetry induced by the Bravais lattice associated with the crystalline phase stable at the applied external temperature and loading conditions (see *e.g.* (Vedantam and Abeyaratne, 2005), or the enlightening reference texts by Pitteri-Zanzotto (Pitteri and Zanzotto, 2003) and Bhattacharya (Bhattacharya, 2003)). These works originate from two fundamental hypotheses: first, the Born rule (lattice vectors deform according to the deformation gradient (Zanzotto, 1996)) is assumed to stand; second, single-grain crystals are considered instead of multi-grain materials, to support the assumption that the relaxed orientation of the lattice vectors remains uniform within the domain or interest. In most applications, however, multi-grain materials are to be used (Casciati and van der Eijk, 2008). When this is the case, macroscopic theories come into play to predict the material response of homogenized samples (Souza et al., 1998; Auricchio and Petrini, 2004a; Hartl et al., 2010), where homogenization arises from the random relative orientation of single SMA grains (we refer the reader to the text by Lagoudas (Lagoudas, 2008) for a clear introduction on the topic).

A crucial subject when focusing on possible engineering applications is the ability to predict the onset of structural and functional fatigue in the material during cyclic transformations (Eggeler et al., 2004). The second task has been attacked by Auricchio and co-workers (Auricchio et al., 2007), by suitably modifying the Souza-Auricchio model (Souza et al., 1998; Auricchio and Petrini, 2004a) of homogenized shape memory alloys. It is the aim of the present paper to proceed further in the direction of introducing a fatigue descriptor in the Souza-Auricchio model. The key element of novelty in our proposal is the formalization of the experimental observation that fatigue effects are intrinsically irreversible

* Corresponding author.
E-mail addresses: noemi.barrera@polimi.it (N. Barrera), paolo.biscari@polimi.it (P. Biscari), marco_urbano@saes-group.com (M.F. Urbano).

(Hornbogen, 2004), and therefore may not be erased by, *e.g.*, simply subjecting the material to an opposite load. Moreover, we also modify the elastic energy, to account for the onset of macroscopic plasticity. In the following, we present and discuss in detail both the Souza-Auricchio model and its proposed modifications. The comparison between the outcome of numerical simulations and experimental results allows us to test the quality of the theoretical predictions.

The paper is organized as follows. In the next section we fix the notations and briefly review the main features of the Souza-Auricchio model of shape memory alloys. In Section 3 we introduce and discuss the main elements of novelty of our approach. In Section 4 we test the model in a model experiment, while in the concluding section we collect the discussion of the results, and the possible developments of the theory.

2. Souza-Auricchio SMA model

We consider shape memory alloys as continua exhibiting inelastic response (Rajagopal and Srinivasa, 1998a, 1998b). More specifically, the setup we present in this section is the Souza-Auricchio model (Souza et al., 1998; Auricchio and Petrini, 2004a), with the plasticity description introduced in Auricchio et al. (2007). Constitutive elements in this thermo-mechanical model are the following.

- The macroscopic strain $\boldsymbol{E}$, defined in terms of the deformation gradient $\boldsymbol{F}$ as $\boldsymbol{E} = 1/2(\boldsymbol{F}^T\boldsymbol{F} - \boldsymbol{I})$, where $\boldsymbol{I}$ is the identity tensor. We further introduce the spherical and deviatoric parts of $\boldsymbol{E}$ by letting $\boldsymbol{E} = \boldsymbol{e} + 1/3E\,\boldsymbol{I}$, with $E = \mathrm{tr}\,\boldsymbol{E}$.
- The transformation strain tensor $\boldsymbol{e}_{\mathrm{tr}}$, and the functional fatigue tensor $\boldsymbol{q}$. The former describes the microstructural transformations. More specifically, it models the presence of a non-zero natural strain, induced by the underlying austenite–martensite phase transitions, in a homogenized material element. Most martensitic transitions, including all self-accommodating transitions, involve small or negligible volume variations (Bhattacharya, 1992). In order to keep our presentation as simple as possible, we therefore focus on isochoric martensitic transformations, though all what follows could be promptly adapted to any volume-changing transformation - as long as the dilation coefficient associated with the transformation is known. In the linearly-elastic regime, an isochoric transformation is characterized by a traceless strain, so that the transformation strain will be represented by a traceless tensor. The functional fatigue $\boldsymbol{q}$ models the irreversible processes induced by microscopic and macroscopic stresses. Increasing $\boldsymbol{q}$ prevents the material from fully recovering from generic external deformations. Evolution of the microscopic order parameters is described through the associated velocity fields

$$\boldsymbol{L}_{\mathrm{tr}} = \dot{\boldsymbol{e}}_{\mathrm{tr}} \quad \text{and} \quad \boldsymbol{L}_q = \dot{\boldsymbol{q}}.$$

- The Piola-Kirchhoff stress tensor $\boldsymbol{S}$, that we will also split as $\boldsymbol{S} = \boldsymbol{s} + 1/3S\,\boldsymbol{I}$, with $S = \mathrm{tr}\,\boldsymbol{S}$.
- The Helmholtz potential density (stored energy function) $\psi(\boldsymbol{E},\boldsymbol{e}_{\mathrm{tr}},\boldsymbol{q};T)$, where T is the absolute temperature. Associated with the Helmholtz potential we introduce the driving forces (Rajagopal and Srinivasa, 1998b; Auricchio et al., 2007)

$$\boldsymbol{X} = -\frac{\partial\psi}{\partial\boldsymbol{e}_{\mathrm{tr}}} \quad \text{and} \quad \boldsymbol{Q} = -\frac{\partial\psi}{\partial\boldsymbol{q}}, \tag{1}$$

that can be shown to be equivalent to the Eshelby configurational forces (Eshelby, 1970) which govern microstructural evolution.

- The rate of dissipation function ξ which, in general, is a function of the microscopic order parameters $\boldsymbol{e}_{\mathrm{tr}},\boldsymbol{q}$, and the related velocity fields $\boldsymbol{L}_{\mathrm{tr}},\boldsymbol{L}_{\mathrm{q}}$. However, by using the maximum rate of dissipation criterion, it can be proved (Rajagopal and Srinivasa, 1998b) that the rate of dissipation depends in fact on the velocity fields only through the driving forces $\boldsymbol{X},\boldsymbol{Q}$, so that we will henceforth consider a rate of dissipation density $\xi(\boldsymbol{e}_{\mathrm{tr}},\boldsymbol{q},\boldsymbol{X},\boldsymbol{Q})$.

The Souza-Auricchio SMA model relies on the small-strain (though not necessarily small displacement) approximation (Auricchio and Petrini, 2004a; Leclercq and Lexcellent, 1996). When this is the case, a linear elastic approximation can be used in the stored energy function, with the transformation strain tensor $\boldsymbol{e}_{\mathrm{tr}}$ modeling the natural strain induced by the austenite–martensite phase transition. A further assumption on the microscopic degrees of freedom is that their evolution is *quasi*-static, in the sense of [19, §VI]. In words, we focus on macroscopic processes that occur on time-scales that are much slower than the microscopic relaxation times. Macroscopic evolution occurs then within the inner part, or at most the boundary, of the elastic domain (the domain over which the rate of dissipation is non-positive). Consequently, evolution of the microscopic order parameters occurs along the boundary of the elastic domain itself.

The Helmholtz potential in Auricchio et al. (2007) can be written as follows

$$\begin{aligned}\psi(\boldsymbol{E},\boldsymbol{e}_{\mathrm{tr}},\boldsymbol{q};T) = {} & \frac{1}{2}KE^2 - 3KE\alpha(T-T_0) + G|\boldsymbol{e}-\boldsymbol{e}_{\mathrm{tr}}|^2 \\ & + \beta\left\langle T - M_{\mathrm{f}}\right\rangle|\boldsymbol{e}_{\mathrm{tr}}-\boldsymbol{q}| + \frac{1}{2}h|\boldsymbol{e}_{\mathrm{tr}}-\boldsymbol{q}|^2 + \frac{1}{2}H|\boldsymbol{q}|^2 \\ & + \vartheta_{\varepsilon_{\mathrm{tr}}}(\boldsymbol{e}_{\mathrm{tr}},\boldsymbol{q}).\end{aligned} \tag{2}$$

The first terms in (2) are proportional to K and G, respectively the bulk and shear modulus. The former penalizes dilations and/or compressions, but for those induced by the thermal expansion coefficient α (not explicitly included in Auricchio et al. (2007), but present in Auricchio and Petrini (2004a)). The latter gives rise to the interpretation of $\boldsymbol{e}_{\mathrm{tr}}$ as relaxed strain. The β-term is temperature dependent and in particular it acts only at temperatures higher than the martensite finish temperature M_{f}, as $\langle\bullet\rangle := \max\{\bullet,0\}$. Effect of this term is to strengthen the effect of the h-term in driving the transformation strain $\boldsymbol{e}_{\mathrm{tr}}$ towards its high-temperature value (austenitic phase), which may be null or not depending on the possible onset of plasticity effects. It is to be noticed the linear vs. quadratic dependence of the β and h terms. Because of this difference the β-term is able to induce a finite driving force even when only a residual transformation strain is left. Finally, the constitutive parameter H models the plastic hardening of the material, and $\vartheta_{\varepsilon_{\mathrm{tr}}}$ is an indicator function that may be null/infinite depending on whether $\boldsymbol{e}_{\mathrm{tr}}$ and $\boldsymbol{q}$ belong to or are outside of the transformation domain $\varepsilon_{\mathrm{tr}}$ that will be discussed in detail below.

The rate of dissipation density proposed in (Auricchio and Petrini (2004a); Auricchio et al. (2007)) admits the following representation in terms of the driving forces

$$\xi(\boldsymbol{X},\boldsymbol{Q}) = \max\{|\boldsymbol{X}| + \kappa|\boldsymbol{Q}| - R, 0\}, \tag{3}$$

where κ is a dimensionless material parameter defining a scaling modulus between fatigue and transformation effects, and R is the radius of the elastic domain (*i.e.*, the domain such that no microscopic evolution takes place until the driving forces reach its boundary).

The transformation domain within which the transformation strain $\boldsymbol{e}_{\mathrm{tr}}$ is forced to evolve, is simply a ball of constant radius ε_{L}

$$\varepsilon_{\rm tr} = \left\{ \boldsymbol{e}_{\rm tr} : \boldsymbol{e}_{\rm tr} = \boldsymbol{e}_{\rm tr}^T,\ {\rm tr}\,\boldsymbol{e}_{\rm tr} = 0, \quad |\boldsymbol{e}_{\rm tr}| \le \varepsilon_L \right\}.$$

The microscopic interpretation of such set is the following. The Souza-Auricchio SMA model aims at modeling a homogenized, multi-grain shape memory alloy where different austenite–martensite transitions may occur in nearby grains. The transformation strain $\boldsymbol{e}_{\rm tr}$ is to be interpreted as the microscopically-induced local natural strain. Now, even if all the local grains are coherently oriented in one and the same direction, the natural strain has an upper bound $\varepsilon_{\rm L}$, which is simply related to the strain associated with the structure of the Bain matrices of the underlying austenite–martensite transition.

Microscopic *quasi*-static evolution is then settled by introducing the flow rules for the internal variables

$$\dot{e}_{\rm tr} = \lambda \frac{\partial \xi}{\partial \boldsymbol{X}}, \quad \dot{q} = \lambda \frac{\partial \xi}{\partial \boldsymbol{Q}}. \tag{4}$$

and the Karush–Kuhn–Tucker conditions related to the dissipation function

$$\lambda \ge 0, \quad \xi = 0, \quad \{\lambda = 0 \quad \text{whenever} \quad |\boldsymbol{X}| + \kappa |\boldsymbol{Q}| < R\}, \tag{5}$$

where the latter condition implements in the present setting the classical yield criterion for the emergence of microstructural modifications.

3. Functional fatigue description in the Souza-Auricchio SMA model

In this section we propose and discuss some improvements that may be of help in bringing the theoretical estimates closer to the experimental results. The main elements of novelty may be summarized as follows: inclusion of macroscopic plasticity in the elastic strain energy; evolution of the transformation strain; introduction of a suitably-modified rate of dissipation function.

3.1. Macroscopic plasticity

When plastic deformations occur, the sample is not able to fully recover the strains induced by arbitrary loads. Let us denote by $\boldsymbol{e}_{\rm el}$ the (traceless part of the) strain which is associated with the elastic energy, and therefore is fully recovered during unloading processes. In the presence of plastic deformations, a plastic strain $\boldsymbol{e}_{\rm pl}$ must be introduced such that

$$\boldsymbol{e}_{\rm el} = \boldsymbol{e} - \boldsymbol{e}_{\rm tr} - \boldsymbol{e}_{\rm pl},$$

where $\boldsymbol{e}$ and $\boldsymbol{e}_{\rm tr}$ are still defined as in the preceding section. Such elastic strain is to be inserted in the shear elastic term in the Helmholtz potential (2). A complete, though maybe unnecessarily involved, theory should provide for a constitutive prescription for the evolution of the plastic strain $\boldsymbol{e}_{\rm pl}$. We prefer, however, to keep the model as simple as possible, and assume the plastic strain to be proportional to the functional fatigue tensor $\boldsymbol{q}$: $\boldsymbol{e}_{\rm pl} = a\,\boldsymbol{q}$. An important feature we do not want to miss is that in shape memory alloys plasticity arises both as a consequence of repeated microscopic phase transitions, and after over-threshold imposed strains. Consequently, it will be necessary (see Section 3.3 below) to modify the functional-fatigue evolution equation to account for possible plastic effects not related to microscopic transformations.

3.2. Evolving transformation domain

The transformation domain aims at modeling the physical effect that, even whenever all the microscopic grains are coherently aligned, the maximum achievable transformation strain is bounded by the size of the Bain matrices associated with the particular austenite–martensite transformation. However, in the presence of functional fatigue effects, *i.e.*, whenever the tensor $\boldsymbol{q}$ undergoes any evolution, it is to be expected that the onset of microscopic defects and dislocations prevents the material from fully aligning in directions different from the one where plasticity is occuring. In other words, increasing values of the functional fatigue tensor model the presence of microscopic domains where phase transitions are not possible anymore, and a fraction of the transformation strain remains *quenched* during subsequent evolution. Consequently, the evolution of $\boldsymbol{q}$ influences the size and shape of the transformation domain $\varepsilon_{\rm tr}$.

We aim at modeling the interpretation of the value of $\boldsymbol{q}$ as the non-recoverable transformation strain at a certain point in space and time. The value of $\boldsymbol{q}$ is therefore to be conceived as the fraction of the initially available transformation strain that remains thenceforth frozen at that specific value. To model this process we put forward an evolution law for the transformation domain $\varepsilon_{\rm tr}$ such that:

- at any point and time, $\varepsilon_{\rm tr}(\boldsymbol{r},t)$ is a ball (in the space of symmetric traceless tensors) centered in $\boldsymbol{q}(\boldsymbol{r},t)$;
- $\varepsilon_{\rm tr}(\boldsymbol{r},t_2) \subseteq \varepsilon_{\rm tr}(\boldsymbol{r},t_1)$ for all $t_2 \ge t_1$;
- $\varepsilon_{\rm tr}(\boldsymbol{r},t)$ is the largest ball among those which satisfy the two preceding criteria.

The following proposition provides an efficient way to completely identify the transformation domain.

Proposition 3.1. *The radius $\varepsilon_{\rm L}$ of the transformation domain evolves along solutions of the differential equation*

$$\dot{\varepsilon}_L(\boldsymbol{r},t) = \begin{cases} -|\dot{\boldsymbol{q}}(\boldsymbol{r},t)| & \text{if } \varepsilon_L(\boldsymbol{r},t) > 0 \\ 0 & \text{if } \varepsilon_L(\boldsymbol{r},t) = 0, \end{cases} \quad \text{with} \quad \varepsilon_L(\boldsymbol{r},t_0) = \varepsilon_{L0}. \tag{6}$$

Proof. Let $\boldsymbol{q}(\boldsymbol{r},t)$ denote the value of the functional fatigue tensor at the material point $\boldsymbol{r}$ at time t (see Fig. 1 for reference). The transformation domain will then be

$$\varepsilon_{\rm tr}(\boldsymbol{r},t) = \left\{ \boldsymbol{e}_{\rm tr} : \boldsymbol{e}_{\rm tr} = \boldsymbol{e}_{\rm tr}^T,\ {\rm tr}\,\boldsymbol{e}_{\rm tr} = 0, \quad |\boldsymbol{e}_{\rm tr} - \boldsymbol{q}(\boldsymbol{r},t)| \le \varepsilon_L(\boldsymbol{r},t) \right\}.$$

When $\boldsymbol{q}$ evolves (say, from $\boldsymbol{q}^{\rm old}$ to $\boldsymbol{q}^{\rm new}$ as illustrated in Fig. 1), we need to identify the largest ball, among those centered in $\boldsymbol{q}^{\rm new}$, which is completely within $\varepsilon_{\rm tr}^{\rm old}$. The radius of such ball is clearly to be decreased (with respect to $\varepsilon_{\rm L}^{\rm old}$) exactly by the amount $\left|\boldsymbol{q}^{\rm new} - \boldsymbol{q}^{\rm old}\right|$. When passing to differential evolution, Equation $(6)_1$ is thus easily recovered. Evolution of the transformation domain ends when the domain itself is turned to a point ($\varepsilon_{\rm L} = 0$).

□

It is important to stress that, in view of the choice of evolution for the transformation domain, any change in the functional fatigue tensor $\boldsymbol{q}$ yields irreversible effects. Indeed, if $\boldsymbol{q}(\boldsymbol{r},t) \neq \boldsymbol{0}$ at any given position and time, the transformation domain at that position will be reduced forever, even if during the future evolution $\boldsymbol{q}$ were to return to its initial null value.

3.3. Rate of dissipation function

Our final proposed modification with respect to the Souza-Auricchio SMA model concerns the rate of dissipation function. The choice we put forward differs from the original proposal (3) in order to extend the validity of the modeling predictions to

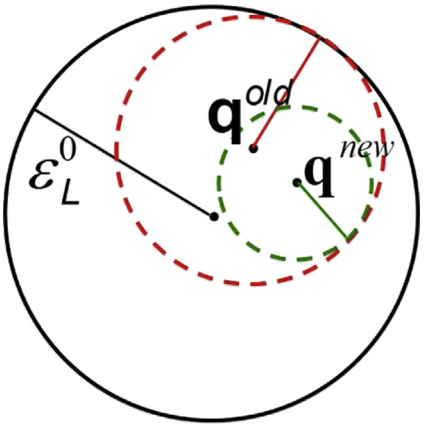

Fig. 1. Representation of the evolution of the transformation domain. Any change in the functional fatigue tensor automatically turns into a reduction of the radius of the transformation domain.

situations in which functional fatigue may arise as a consequence of recoverable transformation strains and/or irreversible plastic strains (Hartl and Lagoudas, 2009).

We begin by associating to any rate of dissipation function a weighted norm $\|\cdot\|_\kappa$, defined on the pairs $(\boldsymbol{X},\boldsymbol{Q})$ such that, for example, the Souza-Auricchio rate of dissipation function can be written as $\xi_1 = \max\{\|(\boldsymbol{X},\boldsymbol{Q})\|_{\kappa,1} - R, 0\}$, where $\|(v_1,v_2)\|_{\kappa,1} = |.v_1|. + \kappa|.v_2|.$ is a weighted ℓ_1 (or taxicab) norm for any strictly positive value of κ. In the following we analyze the consequences of replacing ξ_1 with one of the following choices

$$\xi_2 = \max\Big\{\|(\boldsymbol{X},\boldsymbol{Q})\|_{\kappa,2} - R, 0\Big\},$$
$$\text{where} \|(v_1,v_2)\|_{\kappa,2} = \sqrt{|v_1|^2 + \kappa^2|v_2|^2}$$
(weighted ℓ_2 or Euclidean norm)

$$\xi_\infty = \max\Big\{\|(\boldsymbol{X},\boldsymbol{Q})\|_{\kappa,\infty} - R, 0\Big\},$$
$$\text{where} \|(v_1,v_2)\|_{\kappa,\infty} = \max\{|v_1|, \kappa|v_2|\}$$
(weighted ℓ_∞ or supremum norm).

An immediate consequence of changing the definition of the rate of dissipation function can be promptly understood with the aid of Fig. 2. Modifying the norm in ξ naturally changes the shape of the elastic domain, which is the 0-level set of the rate of dissipation function. More importantly, the direction of the unit normal to the boundary of the domain changes along the boundary itself, and this fact bears nontrivial consequences. Indeed, in the *quasi*-static regime the microscopic variables evolve if and only if the driving forces reach the boundary of the elastic domain. When this happens, $(\dot{\boldsymbol{e}}_{\rm tr}, \dot{\boldsymbol{q}})$ is parallel to the unit normal of the elastic domain (see (4)). The main difference between the proposed choices stems precisely from the relative magnitude of these derivatives.

- When the weighted taxicab norm is chosen, the unit normal to the boundary determines a fixed angle ϕ (precisely $\phi = \arctan\kappa$) with the $|\boldsymbol{X}|$ axis. Suppose now that the model is used with the aim of simulating the material response to, *e.g.*, a thermal cycle along which repeated austenite–martensite transitions are induced. In order for microscopic transitions to occur, the transformation strain $\boldsymbol{e}_{\rm tr}$ must repeatedly evolve from austenite to martensite values. Such evolution occurs if and only if the driving forces repeatedly reach the boundary of the elastic domain. On the other hand, evolution of $\boldsymbol{e}_{\rm tr}$ is automatically coupled with evolution of the functional fatigue tensor. More precisely, since (along the boundary)

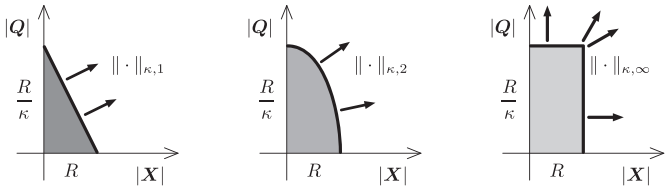

Fig. 2. Different rate of dissipation functions induce different elastic domains, and consequently give rise to different microscopic evolutions. In all plots, the scaling modulus κ has been set equal to 1/2.

$$\frac{\partial\xi_1}{\partial\boldsymbol{X}} = \frac{\boldsymbol{X}}{|\boldsymbol{X}|} \quad \text{and} \quad \frac{\partial\xi_1}{\partial\boldsymbol{Q}} = \kappa\frac{\boldsymbol{Q}}{|\boldsymbol{Q}|},$$

Equation (4) implies that $|\dot{q}| = \tan\phi|.\dot{\boldsymbol{e}}_{\rm tr}|. = \kappa|.\dot{\boldsymbol{e}}_{\rm tr}|.$. In words, any microscopic transformation is necessarily accompanied by an increase in functional fatigue. This prediction is not in agreement with experimental evidence, which claims that after a limited number of cycles (*training* of the sample (Liu et al., 1999; Auricchio et al., 2003)), the stress-strain experimental plots associated with repeated thermal loadings remain basically unchanged for up to thousands of cycles (Van Humbeeck, 1991; Hornbogen, 2004).

- Choosing the Euclidean norm in ξ_2 solves the modeling problem illustrated above. Indeed, the angle ϕ introduced above varies now along the boundary of the elastic domain. The stable cyclic behavior reported after the initial training may then be modeled as follows. As the training process concludes, the system gets to the boundary of the elastic domain with vanishing values of $|\boldsymbol{Q}|$ (*i.e.*, close to the horizontal axis in Fig. 2), so that in such regime $|\dot{\boldsymbol{e}}_{\rm tr}| \gg |\dot{\boldsymbol{q}}|$ as expected. If, on the contrary, in a loading experiment we keep pulling a sample beyond the point where all the material is in the martensitic phase, another interesting phenomenon takes place. Once the transformation strain reaches the boundary of the transformation domain $\varepsilon_{\rm tr}$, the indicator function in (3) comes into play, with the immediate effect of keeping the associated driving force $\boldsymbol{X}$ within the elastic domain. If we, however, keep stretching the specimen, the driving force $\boldsymbol{Q}$ keeps increasing. Eventually the driving forces may reach the boundary of the elastic domain very close to the point $(|.\boldsymbol{X}|., |.\boldsymbol{Q}|.) = (0, R/\kappa)$. When this is the case, the material undergoes macroscopic plasticity without exhibiting any further microscopic phase transformation, as the boundary unit normal has vanishing component along $|\boldsymbol{X}|$.
- The supremum choice associated with ξ_∞ shares all the features we have analyzed in the Euclidean case, but introduces a further degree of freedom, as in practice it introduces two different thresholds (R and R/κ, respectively) for the two driving forces in order for either phase transformation and/or functional fatigue to arise. Both phenomena may, at this point, appear either separately (when one side of the elastic domain is reached) or combined (if the driving forces drive the system to the upper-right corner of the rectangle displayed in Fig. 2). More precisely, Equations (4) and (5) are to be modified in this case by introducing a second Lagrange multiplier μ and setting.

$$\dot{\boldsymbol{e}}_{\rm tr} = \lambda\boldsymbol{X} \quad \text{if } |\boldsymbol{X}| \geq R \quad (\lambda \geq 0), \quad \dot{\boldsymbol{e}}_{\rm tr} = 0 \quad \text{otherwise}$$
$$\dot{\boldsymbol{q}} = \mu\boldsymbol{Q} \quad \text{if } \kappa|\boldsymbol{Q}| \geq R \quad (\mu \geq 0), \quad \dot{\boldsymbol{q}} = 0 \quad \text{otherwise}.$$

4. Thermally-induced hysteresis loops

The Souza-Auricchio SMA model, either in its original form or with the modifications we are discussing in this paper, introduces a

number of constitutive parameters that must be measured experimentally. To this aim we discuss in this section a very simple experiment, in which the role played by the different parameters may be singled out from simple stress-strain measurements performed during repeated uniaxial loadings.

We study the equilibrium configurations of a SMA specimen subject to either uniaxial traction or compression, under uniform temperature conditions. Subsequent equilibrium configurations are obtained by relaxing in a *quasi*-static process the system after infinitesimal loading or temperature variations. We assume that all induced deformations and phase transformations comply with uniaxial symmetry, and that all deformations are homogeneous (affine). In most of the following tests a constant load is applied, and we study the system evolution under cyclic temperature variations, which bring the system across the martensite finish temperature M_f.

The homogeneity assumptions on both the material properties and the deformation guarantee that the momentum balance equation

$$\operatorname{div} \boldsymbol{S} = \boldsymbol{0} \tag{7}$$

is satisfied, the uniform stress tensor being established by the boundary conditions. We stress that we are interested in studying a *quasi*-static process, in which the external control parameters are varied very slowly with respect to the material relaxation times. It is for this reason that we solve the equilibrium Equation (7), while still considering a time evolution (see (4) and (5)) of the microscopic transformation and functional fatigue tensors, under the effect of the driving forces (1). The system of equations is completed by deriving the Piola–Kirchhoff stress tensor $\boldsymbol{S} = \boldsymbol{s} + 1/3S\,\boldsymbol{I}$ from the Helmholtz potential (2) through

$$S = \frac{\partial \psi}{\partial E}, \quad \boldsymbol{s} = \frac{\partial \psi}{\partial \boldsymbol{e}}. \tag{8}$$

The results we discuss below evidence the existence of a hysteresis loop in the macroscopic strain as a function of the temperature. This is a consequence of the fact that the equations we consider admit multiple solutions. The physically relevant one is singled out at each step through continuity requirements. We investigate the shape memory effect of the material by acting upon it with the following thermal cycle. We apply a constant uniaxial load on the specimen at a temperature where only the austenite phase is stable, and start cooling it. At a certain temperature the driving force $|\boldsymbol{X}|$ reaches the critical value, and the austenite–martensite transformation begins. Because of the applied load, the transition is completed at a temperature $T_1 > M_f$. If we now reverse the process, and start increasing the temperature, the reverse transition takes place at a temperature $T_2 > T_1$, because the driving force $\boldsymbol{X}$ must reach a different point of the boundary of the elastic domain (more precisely, the point in the direction of decreasing the transformation strain). It is in this high-temperature, complete transformation interval $T \in [T_1, T_2]$ that plasticity effects are most likely to occur, as the functional fatigue tensor $\boldsymbol{q}$ is most pushed towards the transformation strain $\boldsymbol{e}_{tr}$. This effect reflects the experimental observation that pushing a martensitic transformation up to its complexion often results in a reduction of the fatigue life of the material (Bertacchini et al., 2003, 2009). Subsequent cycles (performed under the same or a reversed applied load) are then possibly influenced by the modified value of the functional fatigue tensor.

Under the symmetry considerations already discussed, all the traceless symmetric tensors $\boldsymbol{s}$, $\boldsymbol{e}$, $\boldsymbol{e}_{tr}$, $\boldsymbol{q}$, $\boldsymbol{X}$, and $\boldsymbol{Q}$ are proportional to one particular tensor, namely $\boldsymbol{i} = \boldsymbol{e}_z \otimes \boldsymbol{e}_z - 1/3\boldsymbol{I}$, where $\boldsymbol{e}_z$ is the direction of the uniaxial loading. We then write $\boldsymbol{s} = s\,\boldsymbol{i}$, $\boldsymbol{e} = e\,\boldsymbol{i}$, $\boldsymbol{e}_{tr} = e_{tr}\,\boldsymbol{i}$, $\boldsymbol{q} = q\,\boldsymbol{i}$, $\boldsymbol{X} = X\,\boldsymbol{i}$, $\boldsymbol{Q} = Q\,\boldsymbol{i}$, and use Equation (8) to obtain

$$\begin{aligned} E &= \tfrac{S}{K} + 3\alpha(T - T_0), \quad s = 2G(e - e_{tr} - aq) \\ X &= s + h(q - e_{tr}) + \left(\gamma + \beta\left\langle T - M_f \right\rangle\right)\operatorname{sgn}(q - e_{tr}) \\ Q &= as + h(e_{tr} - q) - Hq + \beta\left\langle T - M_f \right\rangle \operatorname{sgn}(e_{tr} - q). \end{aligned} \tag{9}$$

Microscopic evolution takes place whenever the driving forces bring the system in contact with the boundary of the elastic domain. When this is the case, e_{tr} and q evolve (with continuity), according to the evolution laws (4), (5).

4.1. Parameter calibration

In any constitutive model it is of paramount importance to identify a small number of easily reproducible experimental tests able to calibrate the value of the relevant phenomenological parameters. To this aim, we now extend to the functional-fatigue case the method put forward in Auricchio et al. (2009) to study the reversible case. Fig. 3 shows the results of repeated cycles performed with the choice of the rate of dissipation function ξ_∞, based on the weighted supremum norm for the driving forces (X,Q), though qualitatively similar results could be obtained with the Euclidean choice ξ_2. We apply on the sample a load s at a temperature where only austenite is stable (point A in the figure). When cooling, phase transformation starts (point B) at the temperature T_B such that

$$X = s - \beta\left(T_B - M_f\right) = R \quad \Rightarrow \quad T_B = M_f + \frac{s - R}{\beta}. \tag{10}$$

It is in particular possible to derive the value of the constitutive parameter β by measuring the value of T_B for different values of the applied load s, as β simply provides (the inverse of) the slope of the T_B *vs* s line. The phase transformation proceeds until $|\boldsymbol{e}_{tr}|$ reaches its maximum allowed value ε_L (point C), which occurs at the temperature

$$s - h\varepsilon_L - \beta\left(T_C - M_f\right) = R \quad \Rightarrow \quad T_C = T_B - \frac{h\varepsilon_L}{\beta}. \tag{11}$$

Since the macroscopic strain (bold line) allows to measure the maximum transformation strain ε_L, a measure of the length of the transformation interval (T_C,T_B) provides an estimate of the ratio h/β (and therefore h). Further cooling of the system (point D) does not yield considerable modifications, though allows to measure the thermal expansion coefficient α. When heating, plastic deformations (point E) first arise when

$$\begin{aligned} Q &= as + h\varepsilon_L + \beta\left(T_E - M_f\right) \\ &= \frac{R}{\kappa} \quad \Rightarrow \quad T_E = T_C + \frac{(1+\kappa)R - (1+a)\kappa s}{\beta\kappa}. \end{aligned}$$

while, neglecting plasticity (as q is expected to be much smaller than ε_L) the reverse transformation occurs in the interval $T \in (T_F, T_G)$, with

$$T_F = T_C + \frac{2R}{\beta} \quad \text{and} \quad T_G = T_B + \frac{2R}{\beta}. \tag{12}$$

The ratio $2R/\beta$ provides then the width of the hysteresis loop. It is interesting to stress that, as long as the functional fatigue parameter q can be neglected when compared to ε_L, the width of the cooling and heating transformation intervals coincide, as $T_G - T_F = T_B - T_C$. The measure of R which follows, together with the T_B value in (10), provides finally the value of the martensite finish temperature M_f.

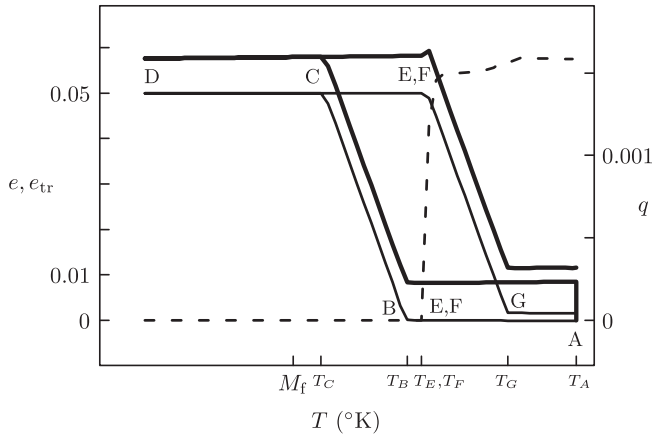

Fig. 3. Evolution of a specimen subject to a thermal cycle across the martensite finish temperature M_f, under a constant uniaxial load s = 150 MPa. The bold line displays the macroscopic strain e, the thin line evidences the transformation strain e_{tr} (both in the left scale), while the dashed plot reports the behavior of the functional fatigue q (in a different scale, illustrated on the right). The value of the constitutive parameters have been set equal to the following realistic values: $K = 34.3$ GPa, $G = 13.2$ GPa, $\alpha = 10^{-5}$/° K, $\beta = 6.71$ MPa/° K, $h = 2$ GPa, $H = 4$ GPa, $\varepsilon_L = 6.12 \times 10^{-2}$, $R = 75.1$ MPa, $\kappa = 0.14$, $a = 0.9$, $M_f = 330°$ K.

4.2. Plasticity and permanent effects

As irreversible evolution is introduced in the model, the response of the material to repeated thermal or mechanical cycles is not periodic. It is the aim of the present section to evidence the role of the modifications to the Souza-Auricchio SMA model proposed in Section 3.

Macroscopic plastic effects enter the Helmholtz potential through the constitutive dimensionless parameter a. As a consequence, performing repeated thermal cycles induces increasing macroscopic deformations, as each attained strain is not fully recovered, and therefore the following thermal cycle pushes farther the deformation. This effect is in turn hindered by both the irreversible shrinking of the transformation domain and the effect of the plastic hardening modulus H. As a consequence, after a certain number of cycles, the *training* (Liu et al., 1999; Auricchio et al., 2003) phase ends and the mechanical response of the sample approaches a periodic limit cycle.

Fig. 4 shows how the plasticity-induced deformation on a thermal cycle depends on the constitutive parameters a (which measures the amount of macroscopic plastic strain induced by the microscopic functional fatigue) and κ (whose value less than 1 models the fact that smaller microscopic driving forces are needed to induce the reversible phase transformation than those necessary to cause fatigue effects). On the y-axis we have reported the difference $\Delta\varepsilon$ between the uniaxial strain when the stationary regime is reached, and the uniaxial strain attained during the first cycle. The plot evidences the existence of a wide range of constitutive parameters for which the linear approximation to the functional dependence $\Delta\varepsilon(a, \kappa)$ provides an excellent prediction. However, a very interesting result is the evidence of the existence of a threshold value under which no plastic effects arise. In other words, if κ and/or a are too small, the loading behavior is reversible, and no plasticity emerges. The reported results for the linear regression predict that plastic effects appear only when $\alpha_1 a + \alpha_2 \kappa + \alpha_3 \geq 0$. By replacing the computed values we obtain $a \geq a_{thr}$, with $a_{thr}(\kappa) = 1.9 - 7.7\kappa$.

The threshold just identified must be expected to depend on the other constitutive parameters as well. It is indeed possible to provide both lower and upper analytical bounds for such a threshold. The analysis of the preceding section showed that in order for plasticity to arise a minimum temperature T_E is to be reached. If such temperature appears to be greater than the temperature T_G at which the reverse transformation is completed, it is plain that no fatigue effect is able to arise. The consequent *necessary* requirement for plastic effects to arise, $T_E \leq T_G$, provides

$$(1 + a)\kappa s \geq (1 - \kappa)R - h\kappa\varepsilon_L \quad \text{(necessary)}.$$

On the other hand a *sufficient* condition for the emergence of plasticity may be obtained by requiring T_E to be lower than the temperature T_F at which the reserve transformation begins. Such condition is equivalent to

$$(1 + a)\kappa s \geq (1 - \kappa)R \quad \text{(sufficient)}.$$

Amid both conditions, the threshold a_{thr} above provides the necessary and sufficient value of a for the emergence of plasticity (in correspondence of the constitutive parameters chosen in Fig. 3).

The effects of the irreversible evolution of the transformation domain are also evidenced if we simulate a different experiment, consisting in repeatedly performing double-cycles in which the material is subject to a thermal cycle (across the martensite finish temperature M_f) under a constant load, and then to an identical thermal cycle under the opposite load. Should a constant transformation domain be assumed, the response of the material to such external conditions would very closely mimic an elastic behavior. Indeed, the functional fatigue tensor $\boldsymbol{q}$ could simply recover during the pushing cycle the null value it abandoned during the pulling phase, paving the way to even a possible cancellation of any trace of the irreversible processes occurring in both stages. In fact, performing repeated double-cycles with constant transformation domain simply results in an overlapping material response.

We have analyzed how the reduction of the transformation domain, and therefore the reduction of the maximum available transformation strain, limits the available strain in repeated double-cycles. Fig. 5 reports how the uniaxial strain lost between the first and second double cycle depends on the modulus κ and the applied load s. As before, the quantity we are computing could in principle depend on all constitutive parameters, but we aim here at underlying the *quasi*-linear behavior which may be obtained for a whole range of values of κ and s. In this case, we have explored higher values of the applied load to evidence the fact that, once the *quasi*-linear regime is abandoned, the system seems to approach a saturation regime in which the lost strain becomes independent of the load.

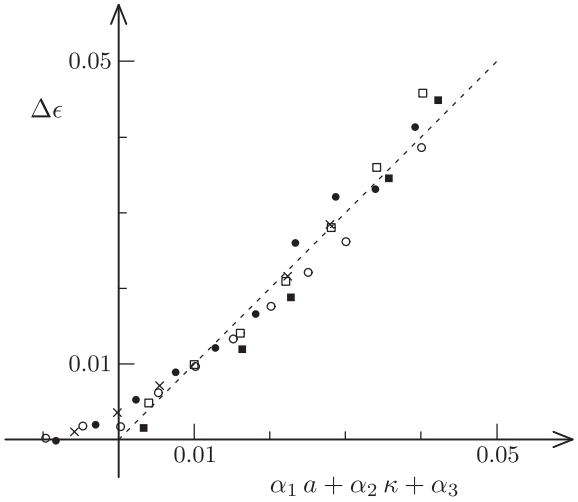

Fig. 4. Plastic deformation as a function of the constitutive parameter a, for different values of κ, namely 0.15 (filled squares), 0.16 (empty squares), 0.17 (crosses), 0.18 (filled circles), and 0.19 (empty circles). The remaining constitutive parameters are as in Fig. 3. The values of the fitting parameters are as follows: $\alpha_1 = 0.10$, $\alpha_2 = 0.81$, $\alpha_3 = -0.20$.

4.3. Comparison with experimental data

In order to test the predictions of the modified Souza-Auricchio SMA model, we have compared the results of the theoretical simulations with the outcome of a practical test. The experiment has been performed in the SAES Getters Laboratories on a TiNi SMA wire (with molar composition of 51%Ti, 49%Ni) with a diameter of 75 μm. The wire is subject to a constant uniaxial stress equal to 360 MPa through the use of a linear motor controlled in closed loop by means of a load cell (Urbano et al., 2008). The initial temperature is sufficiently great to ensure that the system is basically in its austenite phase. The cycle consists in cooling and heating the wire, as previously described in the simulations referring to Fig. 3. Temperature variations are attained by inducing an electric current in the wire, and are controlled through the use of a thermographic camera.

Fig. 6 reports the experimentally-measured strain exhibited by the wire as a function of the temperature, where the features already underlined immediately emerge. The maximum strain induced by the phase transformation increases when repeated cycles are performed, but this growth saturates after a certain number of cycles. This is an evidence of the necessity of introducing the plastic deformation term $a\boldsymbol{q}$ in the elastic part of the Helmholtz potential. On the contrary, no significant effect of the evolution of the transformation domain is to be expected in this test, as our previous study evidenced that such evolution bears critical consequences in double-loading cycles.

In order to test the ability of the model of simulating the experimentally observed behavior, we have calibrated our constitutive parameters to describe the first hysteresis loop in Fig. 6. When performing the comparison, we have used the known material parameters for the bulk and shear moduli. Since we collected data for a single value of the applied load, it was not possible to determine β from the T_B *vs* s slope, as suggested in Section 4.1, and we proceeded by using previous available data on the value of the martensite finish temperature M_f. The value of the uniaxial loading is fixed from the experiment as well. Further material parameters may be directly estimated from the experimental plots: they are the maximum transformation strain ε_L, and the values of the temperatures T_B, T_C, T_F defined in the above section (see Fig. 3). We have further computed the constitutive parameters R, β, h by using Expressions (10), (11), (12). The remaining parameters (*i.e.*, a, κ, and H) have been estimated by fitting the experimental data. The results obtained are summarized in Table 1. Fig. 7 illustrates the outcome, with the experimental points superimposed to the theoretical curves. Though the qualitative agreement is satisfactory, it is plain that no complete matching may be achieved because of the strong simplifying assumptions described at the beginning of the present section. In particular, the difference between the smoothed experimental transition and the abrupt theoretical prediction is certainly to be ascribed to the homogeneity hypothesis introduced in the numerical simulations. In fact, not only the real wire is certainly not homogeneous because of the presence of defects and different grain structure, but also even in the presence of a *quasi*-homogeneous material, the austenite–martensite transition is expected not to occur simultaneously at all places, but rather as a consequence of domain creation and growth. Moreover, it is also to be expected that functional fatigue is not at all homogeneous, as the boundary conditions imposed on the experimental sample may more easily induce functional fatigue close to the hinges and clamps that keep one end of the wire fixed.

5. Conclusions

We have presented and discussed some modifications to be implemented on the Souza-Auricchio macroscopic model for shape memory alloys, with the aim of better reproducing the onset of permanent and functional fatigue effects. The comparison with the experimental data shows a remarkable qualitative agreement, and fosters further studies that may result in a complete characterization of a SMA material in terms of a limited number of parameters, that could then be used for predicting the material response in more complex situations (Auricchio et al., 2009).

The proposed model incorporates the minimal elements necessary to simulate the full fatigue life of a sample, including training, stable regime, and degradation. In order to evidence the three fatigue regimes, let us consider a homogeneous sample undergoing cyclic loading - either thermal or mechanical. At first variations in the transformation strain induce some plastic deformations, mainly induced by the h-term in the Helmholtz potential (2), so that subsequent loading cycles do induce different material responses (see Fig. 3). Both the energy terms proportional to β and h in (2) set the reference value of the transformation strain to be equal to the functional fatigue tensor $\boldsymbol{q}$. Therefore, variations of $\boldsymbol{q}$ during this *training* regime have the effect of paving the way to favor the repetition of similar transformation strain responses in the future. As the cyclic repetitions proceed, the saturation term (proportional to H in the Helmholtz potential) decreases the functional fatigue driving force $\boldsymbol{Q}$ (see also (9)), thus making it harder to hit the yield criterion. We then enter the *stable* regime, where functional fatigue arises at a considerably smaller rate. No matter how slow, functional fatigue continues to appear during the

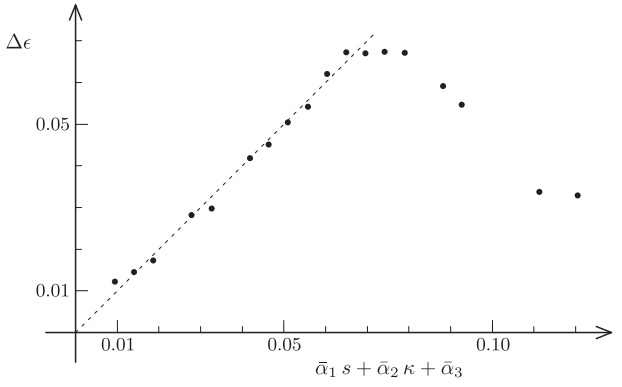

Fig. 5. Lost strain deformation as a function of the constitutive parameter κ (ranging in the interval [0.15,0.17]) and the load s (varying from 3 to 3.1 GPa), for $a = 0.76$. The remaining constitutive parameters are as in Fig. 3. The values of the fitting parameters are as follows: $\bar{\alpha}_1 = 1.83$ GPa^{-1}, $\bar{\alpha}_2 = 4.63$, $\bar{\alpha}_3 = -1.23$.

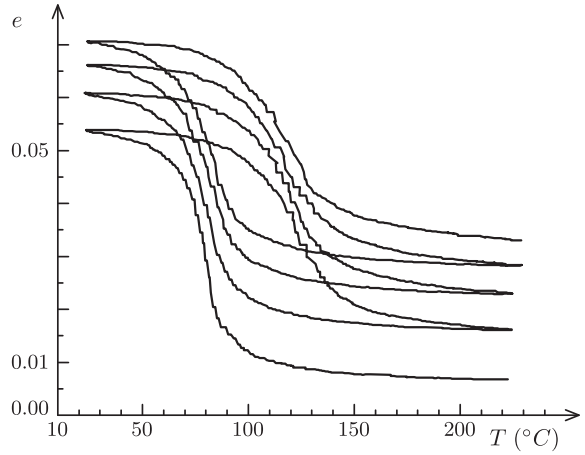

Fig. 6. Experimental results for a TiNi micro-wire, subject to a thermal cycle under a constant uniaxial load, as specified in the text.

Table 1
Values of the constitutive parameters used in Fig. 7.

Parameter	Value	Method
K	60.7 GPa	Known
G	23.3 GPa	Known
M_f	296 K	Known
ε_L	0.0595	Estimated
R	60.6 MPa	Computed
β	3.03 MPa/° K	Computed
h	510 MPa	Computed
a	0.20	Fitted
κ	0.25	Fitted
H	3.7 GPa	Fitted

stable regime (*e.g.*, close to defects and/or clamps in inhomogeneous materials). Therefore, the evolution (6) of the transformation domain eventually reduces it to a point where the transformation strain is not able to trigger the pseudo-elastic behavior anymore. We thus arrive to the *degradation* regime, in which the system is only able to exhibit an elastic response, eventually followed by a plastic slip if the mechanical load increases enough. A quantitative analysis of how the fatigue life predicted by this model compares with respect to experimental evidence will be performed as soon as a sufficient amount of experimental data (covering the three regimes) will become available.

The first assumption to be relaxed is the generalization of the studies here presented to non-homogeneous deformations (Auricchio and Petrini, 2004b; Attanasi et al., 2011). The onset of plastic deformations is indeed a local phenomenon that is to be expected to occur close to points where local stresses increase, such as clamps or inclusions (Urbano, 2012). It is therefore a too restrictive hypothesis to limit the analysis to homogeneous materials and deformations. This generalization does not introduce significant modeling complexity, as the framework remains that of elasto-plastic theories, in the presence of small strains (though not necessarily small displacements). It is however of tantamount importance to study the model cases first, as much more computational power is however required to perform realistic simulations, and few or none analytical estimates are available as soon as complex geometries and/or loads come into play. The study of non-homogeneous processes will further require to relax the hypothesis of uniform temperature and to couple the elasto-mechanical *quasi*-equilibrium equations with the suitable description of heat diffusion (Zanotti et al., 2009).

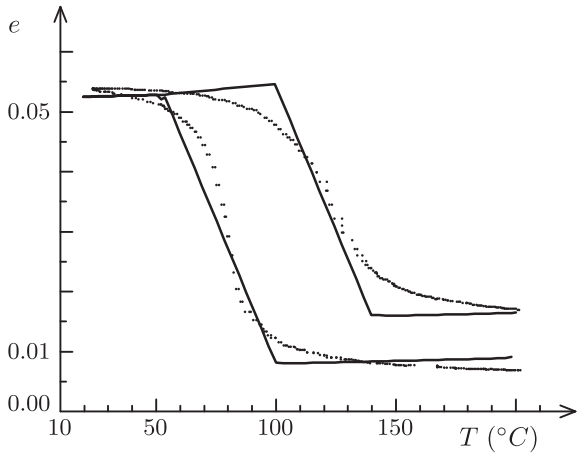

Fig. 7. Comparison of experimental (points) and theoretical (line) results for the first cycle of the TiNi microwire illustrated in Fig. 6, with the constitutive parameters described in the text.

In our study the scaling modulus κ, which enters in the weighted norms that define the rate of dissipation function, has been treated as a constant. We remark, however, that a more accurate description of the macroscopic SMA behavior would likely require an evolution of κ, coupled with the evolution of the transformation domain. It is in particular to be expected that κ should decrease when the radius of the transformation domain does so. In fact, the functional fatigue has been introduced with the aim of modeling the presence within the sample of micro-domains which, as a consequence of the onset of defects and plastic deformations, are no longer able to recover their natural strains. It is therefore to be expected that the more plastic deformations have occurred in a specific material position, the more difficult will be to sum up further plastic effects in the same position.

Acknowledgments

This research has been supported by the Italian Ministry of University and Research Grant No. 200959L72B_004, *"Mathematics and Mechanics of Biological Assemblies and Soft Tissues"*, and by the SAES Getters - Politecnico di Milano research contract *"Microstructural Modeling of Shape Memory Alloys"*.

References

Attanasi, G., Auricchio, F., Urbano, M.F., 2011. Theoretical and experimental investigation on SMA superelastic springs. J. Mater. Eng. Perform. 20, 706–711.
Auricchio, F., Petrini, L., 2004a. A three-dimensional model describing stress-temperature induced solid phase transformations: thermomechanical coupling and hybrid composite applications. Int. J. Numer. Methods. Eng. 61, 716–737.
Auricchio, F., Petrini, L., 2004b. A three-dimensional model describing stress-temperature induced solid phase transformations: solution algorithm and boundary value problems. Int. J. Numer. Methods Eng. 61, 807–836.
Auricchio, F., Marfia, S., Sacco, E., 2003. Modelling of SMA materials: training and two way memory effects. Comput. Struct. 81, 2301–2317.
Auricchio, F., Reali, A., Stefanelli, U., 2007. A three-dimensional model describing stress-induced solid phase transformation with permanent inelasticity. Int. J. Plast. 23, 207–226.
Auricchio, F., Coda, A., Reali, A., Urbano, M.F., 2009. SMA numerical modeling versus experimental results: parameter identification and model prediction capabilities. J. Mater. Eng. Perform. 18, 649–654.
Ball, J.M., James, R.D., 1987. Fine phase mixture as minimizers of energy. Arch. Ration. Mech. Anal. 100, 13–52.
Bekker, A., Brinson, L.C., 1998. Phase diagram based description of the hysteresis behavior of shape memory alloys. Acta Mater. 46, 3649–3665.
Bertacchini, O.W., Lagoudas, D.C., Patoor, E., 2003. Fatigue life characterization of shape memory alloys undergoing thermomechanical cyclic loading. In: Proc. SPIE, San Diego. Smart Structures and Materials: Active Materials: Behavior and Mechanics, vol. 5053, pp. 612–624.
Bertacchini, O.W., Lagoudas, D.C., Patoor, E., 2009. Thermomechanical transformation fatigue of TiNiCu SMA actuators under a corrosive environment – Part I: experimental results. Int. J. Fatigue 31, 1571–1578.
Bhattacharya, K., 1992. Self-accommodation in martensite. Arch. Ration. Mech. Anal. 120, 201–244.
Bhattacharya, K., Conti, S., Zanzotto, G., Zimmer, J., 2004. Crystal symmetry and the reversibility of martensitic transformations. Nature 428, 55–59.
Bhattacharya, K., 2003. In: Microstructure of Martensite: Why it Forms and how it Gives Rise to the Shape Memory Effect?. Oxford University Press.
Casciati, F., van der Eijk, C., 2008. Variability in mechanical properties and microstructure characterization of CuAlBe shape memory alloys for vibration mitigation. Smart Mater. Struct. 4, 103–121.
Eggeler, G., Hornbogen, E., Yawny, A., Heckmann, A., Wagner, M., 2004. Structural and functional fatigue of NiTi shape memory alloys. Mater. Sci. Eng. A Struct. 378, 24–33.
Eshelby, J.D., 1970. Energy relations and the energy momentum tensor in continuum mechanics. In: Kanninen, M.F. (Ed.), Inelastic Behaviour of Solids. McGraw-Hill, New York, U.S.A., pp. 77–115.
Hartl, D.J., Lagoudas, D.C., 2009. Constitutive modeling and structural analysis considering simultaneous phase transformation and plastic yield in shape memory alloys. Smart Mater. Struct. 18. #104017.
Hartl, D.J., Chatzigeorgiou, G., Lagoudas, D.C., 2010. Three-dimensional modeling and numerical analysis of rate-dependent irrecoverable deformation in shape memory alloys. Int. J. Plast. 26, 1485–1507.
Hornbogen, E., 2004. Thermo-mechanical fatigue of shape memory alloys. J. Mater. Sci. 39, 385–399.

Lagoudas, D.C., 2008. In: Shape Memory Alloys: Modeling and Engineering Applications. Springer-Verlag.
Leclercq, S., Lexcellent, C., 1996. A general macroscopic description of the thermomechanical behavior of shape memory alloys. J. Mech. Phys. Solids 44, 953–980.
Liu, Yi., Liu, Yo., Van Humbeeck, J., 1999. Two-way shape memory effect developed by martensite deformation in NiTi. Acta Mater. 47, 199–209.
Otsuka, K., Ren, X.B., 1999. Recent developments in the research of shape memory alloys. Intermetallics 7, 511–528.
Pitteri, M., Zanzotto, G., 2003. In: Continuum Models for Phase Transitions and Twinning in Crystals. Chapman & Hall.
Rajagopal, K.R., Srinivasa, A.R., 1998a. Mechanics of the inelastic behavior of materials – Part I, theoretical underpinnings. Int. J. Plast. 14, 945–967.
Rajagopal, K.R., Srinivasa, A.R., 1998b. Mechanics of the inelastic behavior of materials – Part II, inelastic response. Int. J. Plast. 14, 969–995.
Shabalovskaya, S., Anderegg, J., Van Humbeeck, J., 2008. Critical overview of nitinol surfaces and their modifications for medical applications. Acta Biomater. 4, 447–467.
Souza, A.C., Mamiya, E.N., Zouain, N., 1998. Three-dimensional model for solids undergoing stress-induced phase transformations. Eur. J. Mech. A Solids 17, 789–806.
Urbano, M.F., 2012. Study of the influence of inclusions on the behavior of NiTi shape-memory alloys in thermal cycling by means of finite element method. Metall. Mater. Trans. A 43, 2912–2920.
Urbano, M., Coda, A., Giannantonio, R., 2008. SMAq: a novel integrated instrument for the characterization of SMA wires. In: Berg, B., Mitchell, M.R., Proft, J. (Eds.), SMST 2006 (Int. Conf. on Shape Memory and Superelastic Technologies) Proceedings, pp. 177–184.
Van Humbeeck, J., 1991. Cycling effects, fatigue and degradation of shape memory alloys. J. Phys. IV France 1, 189–197.
Vedantam, S., Abeyaratne, R., 2005. A helmholtz free-energy function for a CuAlNi shape memory alloy. Int. J. Non Linear. Mech. 40, 177–193.
Zanotti, C., Giuliani, P., Riva, G., Tuissi, A., Chrysanthou, A., 2009. Thermal diffusivity of Ni-Ti SMAs. J. Alloys. Compd. 473, 231–237.
Zanzotto, G., 1996. The Cauchy-Born hypothesis, nonlinear elasticity and mechanical twinning in crystals. Acta Cryst. A 52, 839–849.